Isomerization of α-pinene oxide using Fe-supported catalysts: Selective synthesis of campholenic aldehyde

Martina Stekrova [a,b,c], Narendra Kumar [a], Atte Aho [a], Ilia Sinev [d], Wolfgang Grünert [d], Johnny Dahl [e], Jorma Roine [e], Sergey S. Arzumanov [f], Päivi Mäki-Arvela [a], Dmitry Yu. Murzin [a,*]

[a] Laboratory of Industrial Chemistry and Reaction Engineering, Åbo Akademi University, FI-20500 Turku, Finland
[b] Institute of Chemical Technology Prague, Department of Organic Technology, Prague 6, Czech Republic
[c] Research Institute of Inorganic Chemistry, Inc., Ústí nad Labem, Czech Republic
[d] Ruhr University Bochum, Germany
[e] Department of Physics and Astronomy, University of Turku, Turku, Finland
[f] Boreskov Institute of Catalysis, Novosibirsk, Russia

ARTICLE INFO

ABSTRACT

α-Pinene oxide, an oxygenated derivative of α-pinene, can be converted into various valuable substances useful as flavour, fragrance and pharmaceutical compounds. Campholenic aldehyde is one of the most desired products of α-pinene oxide isomerization being a valuable intermediate for the production of sandalwood-like fragrances. Iron modified zeolites Beta-75 and ZSM-5, mesoporous material MCM-41, silica and alumina were prepared by two methods (impregnation and solid-state ion exchange) and tested for selective preparation of campholenic aldehyde by isomerization of α-pinene oxide. The characterization of tested catalyst was carried out using scanning electron microscope analysis, nitrogen adsorption measurements, pyridine adsorption–desorption with FTIR, X-ray absorption spectroscopy measurements, XPS-analysis, ^{29}Si MAS NMR and ^{27}Al MAS NMR and X-ray diffraction. The isomerization of α-pinene oxide was carried out in toluene as a solvent at 70 °C. The main properties influencing the activity and the selectivity are the acidic and structural properties of the tested catalysts. The highest selectivity of 66% was achieved at complete conversion of α-pinene oxide with Fe-MCM-41.

© 2013 Elsevier B.V. All rights reserved.

1. Introduction

Terpenic compounds are an interesting renewable feedstock for the production of fragrances and pharmaceuticals [1–17]. Their oxygenated derivatives form one of the most important groups of fragrance ingredients. α-Pinene is a biomass derived substrate that can be obtained from turpentine oil, being a valuable raw material for the production of compounds further used in the fine chemical industry. Its oxygenated derivative, α-pinene oxide, can be converted in various substances useful as flavour, fragrance and pharmaceutical compounds. Campholenic aldehyde is the most desired product of α-pinene oxide isomerization because it is an intermediate for the production of sandalwood fragrance, santalol.

The rearrangement of α-pinene oxide yields various aldehydes and alcohols by acid catalysis (Fig. 1). This reaction can be homogeneously catalyzed by Lewis acids, and a conventional process based

on zinc bromide gives the selectivity to campholenic aldehyde 85% [4–6].

To be more environmentally benign, there is a trend for heterogenization of the processes using solid acid catalysts. Several articles have been published focusing on the influence of Lewis and Brønsted acid sites of heterogeneous catalysts in this reaction [7–17]. In addition to metal salt catalysts supported on oxide [10] or zeolites [7,15] also crystalline metal organic framework catalysts composed of $Cu_3(btc)2$, benzene-1,3,5-tricarbolyxate have been used in the isomerization of α-pinene oxide [9] giving 87% selectivity of campholenic aldehyde in acetonitrile at 25 °C. Furthermore, a zinc complex, $Zn(Otf)_2$ supported on silica gave 65% selectivity to campholenic aldehyde at complete conversion of α-pinene oxide in dichloromethane at 85 °C [12]. Even B_2O_3/SiO_2 was quite selective to campholenic aldehyde (69%) at 84% conversion in toluene at room temperature [13]. Dealuminated zeolite H-US-Y was reported to afford selectivity of about 78% to campholenic aldehyde at 0 °C [7]. Zeolite titanium Beta was found to be an effective catalyst for rearrangement of α-pinene oxide to campholenic aldehyde, giving selectivity up to 89% [8]. Isomerization of α-pinene oxide has been investigated over an oxide catalyst containing highly dispersed Fe
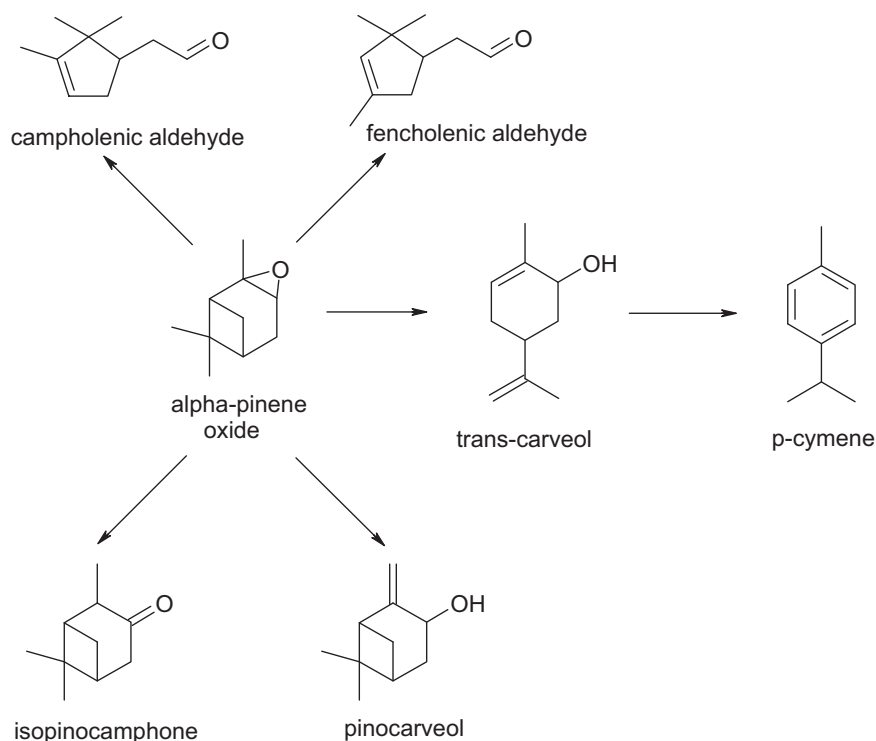
Fig. 1. Reaction scheme of α-pinene oxide isomerization to campholenic and fencholenic aldehyde to *trans*-carveol and *p*-cymene and to pinocarveol and isopinocamphone.

phases supported on mesoporous silica [14]. The formation of campholenic aldehyde was observed to be influenced by the presence of Lewis acid sites as well as the presence of iron. The selectivity to campholenic aldehyde was around 53% in toluene at room temperature [14]. Ravasio et al. investigated Fe supported onto pure silica and series of modified silicas with variable amount of zirconia [16] Total conversion of α-pinene oxide with 65% selectivity to campholenic aldehyde was obtained over Fe/SZ5 (5 wt.% of zirconia) in toluene at room temperature [16]. In addition, in a very recent publication of Coelho et al. [17] it was reported that MCM mesoporous silica containing Fe^{3+} gave 70% selectivity to campholenic aldehyde at 70% conversion in dichloroethane at 40 °C.

In the current study isomerization of α-pinene oxide over several iron supported heterogeneous catalysts was investigated. In this work a wide range of supports with varying structures such as zeolites (ZSM-5 and Beta-75), silica, alumina and MCM-41 were modified by iron, characterized and tested for campholenic aldehyde preparation. The influence of iron loading on silica and alumina to the activity and selectivity of catalysts was investigated. Furthermore, the influence of concentration of Lewis and Brønsted acid sites was elucidated. Two methods of catalyst synthesis were used in this research, namely conventional impregnation method and solid state ion exchange method.

2. Experimental

2.1. Catalyst synthesis

The NH_4-ZSM-5 and NH_4-Beta-75 zeolites were obtained from Zeolyst International. The NH_4^+ forms of zeolites were transformed to proton forms at 500 °C in a muffle oven using a step calcination procedure.

Silica gel (Merck & Co., Inc.) and aluminium oxide (UOP Inc.) were used as other supports.

Mesoporous material MCM-41 was synthesized in the sodium form (Na–MCM-41) using a Parr autoclave (300 mL) as mentioned in [18] with few modifications [19]. After synthesis of MCM-41, it was filtered, washed with distilled water, dried overnight at 100 °C and calcined. Proton form H–MCM-41 was prepared by ion-exchange with ammonium chloride, followed by washing with distilled water, drying and calcination at 450 °C.

Two methods of iron introduction in the catalysts were used, namely conventional impregnation (IMP) and solid state ion exchange methods (SSIE). Ferric nitrate ($Fe(NO_3)_3 \cdot 9 H_2O$, Fluka) was used as an iron precursor in all cases. The impregnation method from aqueous solutions was used for preparation of the following catalysts: Fe-SiO$_2$ IMP and Fe-Al$_2$O$_3$ IMP. The Fe modification of Beta-75, ZSM-5 and H-MCM-41 was performed using solid state ion exchange method.

Loading amount of iron on silica and on alumina was supported using water as a solvent, the mixture was stirred for 24 h at 60 °C. The other steps of synthesis were evaporation, drying at 100 °C overnight and calcination at 450 °C for 4 h. SSIE preparation method was performed without any solvent. The mixture of support and iron precursor was ball-milled for 8 h. The other steps of synthesis were drying (100 °C overnight) and calcination (450 °C, 4 h).

2.2. Catalyst characterization

2.2.1. Scanning electron microscope analysis

Morphological studies were performed by scanning electron microscopy. The scanning electron microscope (Zeiss Leo Gemini 1530) was used for determining the crystal morphology of the proton forms and Fe-modified catalysts.

2.2.2. Nitrogen adsorption measurements

The specific surface areas of supports and of iron modified catalysts were determined by nitrogen adsorption using Sorptometer 1900 (Carlo Erba instruments). The samples were outgassed at 150 °C for 3 h before each measurement. The BET equation was used for calculation of the specific surface area of mesoporous materials

and silica and alumina and the Dubinin's equation was used for calculation of the specific surface area of microporous zeolites.

2.2.3. Pyridine adsorption–desorption with FTIR

The acidity of the proton and Fe modified catalyst was measured by infrared spectroscopy (ATI Mattson FTIR) using pyridine ($\geq$ 99.5%) as a probe molecule for qualitative and quantitative determination of both Brønsted and Lewis acid sites. The samples were pressed into thin pellets (10–25 mg). The pellets were pretreated at 450 °C before the measurement. Pyridine was first adsorbed for 30 min at 100 °C and then desorbed by evacuation at different temperatures. Three different temperatures were used for desorption of pyridine, defined as 250 °C–350 °C as weak, medium and strong sites, 350 °C–450 °C as medium and strong sites as well as pyridine which stays adsorbed after desorption at 450 °C as strong sites [20]. The amount of Brønsted and Lewis acid sites were calculated from the intensities of the corresponding spectral bands, 1545 cm^{-1} and 1450 cm^{-1}, respectively, using the molar extinction parameters previously reported by Emeis [21]. The catalysts weights were taken into account in the calculations.

2.2.4. X-ray absorption spectroscopy measurements

FeK edge (7111 eV) XAS measurements were carried out at HASYLAB on the beamline X1 and on CLÆSS beamline of ALBA synchrotron facility. Si (1 1 1) double crystal monochromator was used for the energy scan along with Rh-coated toroid mirror for unwanted harmonics elimination. The spectra were recorded in the transmission mode at ambient temperature. For the measurements samples were pressed in self supporting pellets and wrapped with Kapton tape. Spectra were measured simultaneously with the reference spectrum Fe foil placed between second and third ionisation chambers, so that the absolute energy calibration is performed. Fe foil and α-Fe$_2$O$_3$ (hematite), which were used as references, were collected at the same conditions. All spectra were measured two times to ensure their reproducibility.

Analysis of the EXAFS spectra was performed with the software VIPER for Windows [22]. In the spectra of the absorption coefficient μ, a Victorian polynomial was fitted to the pre-edge region for background subtraction. A smooth atomic background μ_0 was evaluated using a smoothing cubic spline. The Fourier analysis of k^2-weighted experimental function $\chi = (\mu - \mu_0)/\mu_0$ was performed with a Kaiser window. The required scattering amplitudes and phase shifts were calculated by the *ab initio* FEFF8.10 code [23] for α-Fe$_2$O$_3$ (hematite) structure. The fitting was done in the k- and r-spaces simultaneously. The shell radius r, coordination number N, Debye–Waller factor σ^2 and adjustable "muffin-tin zero" ΔE were determined as fitting parameters. The errors of the fitting parameters were found by decomposition of the statistical χ^2 function near its minimum, taking into account maximal pair correlations.

2.2.5. XPS analysis

The photoemission spectra were measured using a Perkin-Elmer PHI 5400 spectrometer with a monochromatized Al Kα X-ray source that was operated at 14 kV, 300 W. The analyzer pass energy was 17.9 eV and the energy step was 0.1 eV. The vacuum chamber base pressure was 10^{-9} mbar. The use of charge neutralizer was necessary and its power was set so that Si 2p peak was at 103.5 eV, corresponding to SiO$_2$ binding energy. The studied peaks were Fe 2p, Si 2p and Al 2p. Also, a 1400 eV survey spectrum was taken for each sample. The step length was 0.5 eV. The peaks were calibrated using binding energy (BE) of SiO$_2$ which is 103.3–103.7 eV.

2.2.6. ^{29}Si MAS NMR and ^{27}Al MAS NMR

NMR spectra were recorded at 9.4 T on a Bruker Avance-400 spectrometer equipped with broad-band double-resonance-MAS probe. ^{27}Al MAS NMR spectra were acquired with a short $\pi/12$ radio

frequency pulse (0.6 μs), and about 1000 scans were accumulated with a 0.5 s recycle delay. ^{29}Si MAS NMR spectra were recorded with a $\pi/2$ excitation pulse of 5.0 μs duration and 20 s repetition time, and 1000 scans were acquired for signal accumulation. Both ^{27}Al and ^{29}Si NMR spectra were recorded with use of 4 mm rotors and a spinning rate of 10–15 kHz.

2.2.7. X-ray diffraction

Powder X-ray diffraction (XRD) of the samples was measured using Philips X'Pert Pro MPD using monocrhomated CuKα radiation at 40 kV/50 mA. The divergence slit was 0.25° with a fixed 20 mm mask. The diffractograms were analyzed by Philips X'Pert HighScore MAUD programs.

2.3. Catalytic tests

Liquid phase isomerization of α-pinene oxide over the Fe modified catalysts was carried out in the batch-wise operating glass reactor. In a typical experiment using toluene as a solvent (V_L = 150 ml) the initial concentration of α-pinene oxide and the catalyst mass were 0.013 mol/l and 75 mg, respectively. The kinetic experiments were performed at 70 °C under the following conditions to avoid external mass transfer limitation: the catalysts particle size below 90 μm and the stirring speed of 390 rpm. The catalyst was activated in the reactor at 250 °C under an inert argon atmosphere for 30 min before the reaction. The samples were taken at different time intervals and analyzed by GC using a DB-Petro column with a capillary column of 100 m x 250 μm x 0.50 μm nominal (Agilent 128-1056) and with a FID detector. The products were confirmed by GC-MS.

In order to evaluate a possibility of catalyst reuse, the spent catalyst was filtered from the reaction mixture after isomerization, washed by acetone and dried overnight at 100 °C and reused in the reaction. In the case of catalyst regeneration, calcination at 400 °C was done prior to reaction.

3. Results and discussion

3.1. Catalyst characterization

3.1.1. Morphological studies by scanning electron microscopy

The morphology (shape and size) of the Fe modified catalysts were studied by scanning electron microscopy (Figs. 2–5). Fe modification of H-ZSM-5 and H-Beta-75 zeolites did not influence the parent crystal morphology (Fig. 2). No apparent changes in crystal morphology were observed due to the loading various amount of iron on silica in the SEM micrographs (Fig. 4). In the case of 10 wt.% of iron on alumina, changes in the structure of the catalyst were observed (Fig. 5). Fig. 3 compares crystal morphologies of the fresh Fe-MCM-41-SSIE and the catalyst after isomerization. The fresh Fe-MCM-41-SSIE is characterized by uniform particle size distribution (Fig. 3a). On the other hand, the spent catalyst contains larger particles with various sizes which is caused by agglomeration of particles during the reaction. As it is discussed below, the Fe-MCM-SSIE catalyst can be fully regenerated and catalyst activity regained (Table 11). The catalyst deactivation in the isomerization reaction of α-pinene oxide is attributed to the pore blockage of the Fe-MCM-41-SSIE by carbon residuals and not due to morphology changes in MCM-41 or Fe species (Table 2). So there should not be any changes in the morphology or sintering of Fe species, otherwise it would not have been possible to regenerate the catalyst. It can be conclude, that the MCM-41 crystals are kept intact after the isomerization reaction of α-pinene and only reversible agglomeration of catalyst particles occurred during the reaction.
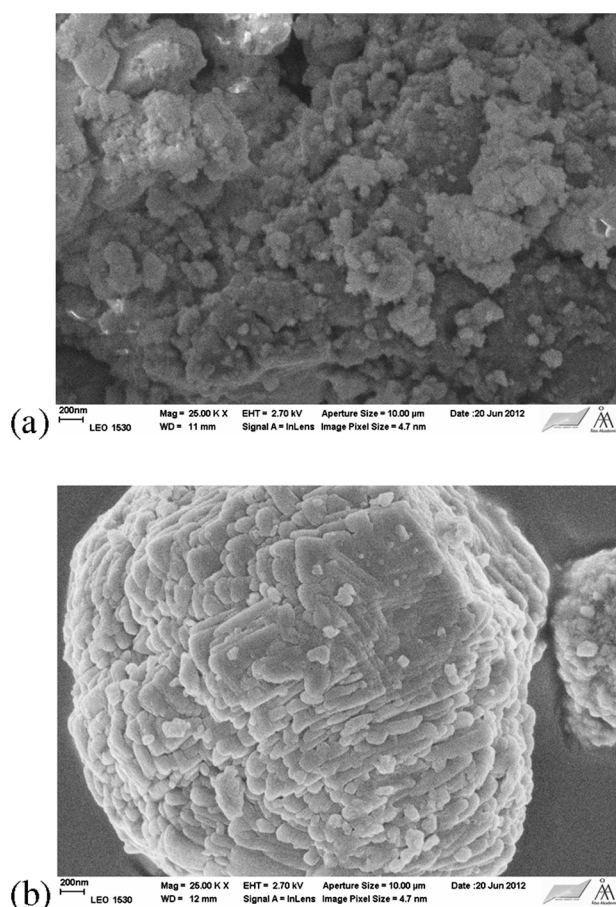
Fig. 2. Scanning electron micrograph of (a) Fe-Beta-75 SSIE and (b) Fe-ZSM-5 SSIE.

Fig. 3. SEM image of Fe-H-MCM-41-SSIE (a) after preparation and (b) after the isomerisation.

Energy dispersive X-ray microanalysis (SEM-EDXA) was performed to measure Fe content in the catalysts. The results are presented in Table 1.

The Fe-modified silica and alumina were prepared to achieve a different metal loading of 3, 5 and 10 wt.%. The EDXA results shown in Table 1 are somewhat lower than this nominal loading. The Fe-modified MCM-41 and Beta-75 were prepared to achieve an iron loading of 3 wt.%. The results given in Table 1 are close to this nominal loading, indicating that the solid state ion-exchange method used for the metal introduction was successful. The same is valid for Fe-ZSM-5 with nominal loading of iron 1 wt.%. Furthermore, EDXA was measured for the spent Fe-H-MCM-41-SSIE (used in the isomerization reaction). The observed slight decrease of the iron content

might be related to leaching of iron during the isomerization reaction.

3.1.2. Specific surface areas of the catalysts

The specific surface areas of the Fe modified catalysts determined by nitrogen adsorption and calculated by BET and Dubinin' methods are summarized in Table 2.

The specific surface areas decrease in the most cases after the metal introduction due to blocking of some micro- or mesopores.

The lowest specific surface areas were determined for Fe-alumina catalysts and the highest one for Fe-MCM-41-SSIE catalyst.

The specific surface area of Fe-MCM-41-SSIE spent catalyst was lower than that of the fresh Fe-MCM-41-SSIE catalyst, which may be attributed to the partial blockage of the pores by carbon residues during the reaction. The regeneration of the catalyst caused again the increase of the specific surface area although the initial value for the fresh Fe-MCM-41-SSIE catalyst could not have been achieved.

3.1.3. X-ray photoelectron spectroscopy results

X-ray photoelectron spectroscopy of the studied catalysts samples was performed (Figs. 6 and 7). The X-ray photoelectron spectroscopy of iron catalysts demonstrated that iron is presented in three oxidation states metallic: Fe^0, low oxidation Fe^{2+} and high oxidation Fe^{3+} according to ref. [25]. The highest amount of Fe^{3+} (50%) was present in Fe-ZSM-5 and Fe-Beta-75, catalysts with no or very small amount of metallic Fe, respectively. The highest amount of metallic Fe^0 being 31% was observed in mesoporous Fe-MCM-41-SSIE catalyst (Table 3). This result should however be taken

Table 1
Iron loading determined by energy dispersive X-ray microanalysis.

Catalyst		Nominal Fe loading (wt.%)	Fe loading determined by SEM-EDXA (wt.%)
Fe-SiO$_2$ IMP		3	2.4
		5	4.6
		10	8.3
Fe-Al$_2$O$_3$ IMP		3	2.8
		5	4.5
		10	7.1
Fe-H-MCM-41 SSIE	Fresh	3	2.9
	Spent		2.1
Fe-Beta-75 SSIE		3	3.1
Fe-ZSM-5 SSIE		1	1.2

Table 2
Properties of Fe-modified catalysts.

Catalyst/support		Nominal iron content (wt %)	Specific surface area (m^2/g)	Pore specific volume (cm^3/g)
SiO$_2$		–	496	0.92
		3	451	0.82
Fe-SiO$_2$ IMP		5	389	0.68
		10	390	0.63
Al$_2$O$_3$		–	303	1.34
		3	268	1.12
Fe-Al$_2$O$_3$ IMP		5	261	1.13
		10	240	0.75
H-MCM-41		–	944 [24]	–
Fe-MCM-41 SSIE	Fresh		807	0.92
	Regenerated	3	678	0.63
	spent		331	0.40
H-Beta-75		–	664	–
Fe-Beta-75 SSIE		3	467	0.59
ZSM-5		–		
Fe-ZSM-5 SSIE		1	552	0.20

Table 3
Characterization results of the oxidation states of Fe supported catalysts by X-ray photoelectron spectroscopy.

	Amount of oxidation states of Fe (%)		
	Fe^0	Fe^{2+}	Fe^{3+}
Fe-Beta-75-SSIE	4	46	50
Fe-ZSM-5-SSIE	0	50	50
Fe-MCM-41SSIE	31	28	41
Fe SiO$_2$ (5 wt.%)-IMP	0	73	27
Fe-SiO$_2$ (10 wt.%)-IMP	0	72	28

with caution, since it is derived from a deconvolution of a noisy XPS signal and moreover there was no reduction made prior to XPS measurements. In any case metallic iron was not observed by EXAFS as will be discussed below.

Iron modified silica is characterized by high content of Fe^{2+}.

3.1.4. Acid site concentrations of the catalysts measured by pyridine adsorption desorption with FTIR

Concentrations of Brønsted and Lewis acid sites were determined by FTIR using pyridine as a probe molecule. The results revealed that the highest total Brønsted acid concentration for iron containing catalysts was obtained for Fe-Beta-75, followed by Fe-ZSM-5. The least Brønsted acid sites were determined for the Fe-SiO$_2$ catalyst with 5 wt.% of loading Fe (Table 4). The Lewis acid site concentrations decreased in a different order compared to Brønsted acid site concentrations. Fe-Beta-75-SSIE and Fe-Al$_2$O$_3$ contained the highest amount of Lewis acid sites. The acidities of catalysts Fe-Al$_2$O$_3$ are dependent on the high amount of Fe. The highest

total Brønsted and Lewis acid concentration were determined for Fe-Beta-75-SSIE.

3.1.5. EXAFS and XANES results

X-ray absorption spectra were recorded for a hematite standard, α-Fe$_2$O$_3$ as well as for Fe-ZSM-5, Fe-MCM-41-SSIE, Fe-Beta-75 and Fe-SiO$_2$ catalysts and the near-edge region of the normalized X-ray absorption spectra for these three catalysts are depicted in Fig. 8.

Fig. 8 shows the near-edge region of the normalized X-ray absorption spectra for the prepared samples as well as α-Fe$_2$O$_3$ for comparison. The edge positions of most samples are quite similar (ca. 7125 eV), indicating that the oxidation state of iron in the samples under study is predominantly +3, as in the reference oxide. In all spectra a pre-edge peak (marked as A) is observed. This peak arises from a 1s → 3d transition, which is forbidden for coordination geometries with an inversion centre. Therefore, the origin of this signal could be iron in tetrahedral or in distorted octahedral coordination. As shown by Wilke and co-authors [28] pre-edge feature position and height can serve as a quantitative indicator for iron oxidation state and coordination geometry. Pre-edge positions are summarized in Table 5 for the samples and hematite. As it can be seen, all samples demonstrate pre-edge position close to that of α-Fe$_2$O$_3$ therefore it can be concluded that iron has predominantly 3+ oxidation state. Relatively higher intensity of those pre-edge signals also indicates that iron is presented in a mixture of 4- and 6-fold coordination geometry. Silica supported sample shows a pre-edge feature centered at 7112.8 eV which indicates that iron is presented in a mixture of Fe^{2+} and Fe^{3+} ions in octahedral coordination. These results are slightly different from those

Table 4
Brønsted and Lewis acidities of the supports and Fe modified catalysts determined by FTIR.

Catalysts		Brønsted acidity (μmol/g)			Lewis acidity (μmol/g)		
		250 °C	350 °C	450 °C	250 °C	350 °C	450 °C
Fe-SiO$_2$ IMP	5 wt.%	4	4	2	5	3	1
Fe-Al$_2$O$_3$ IMP	3 wt.%	9	9	4	133	57	19
	5 wt.%	12	12	6	140	62	12
	10 wt.%	6	5	0	98	45	6
H-MCM-41 [24]		*26*	*11*	*3*	*40*	*20*	*12*
Fe-H-MCM-41 SSIE		22	8	0	45	17	0
H-Beta-75 [26]		*176*	*161*	*72*	*43*	*23*	*10*
Fe-Beta-75 SSIE		193	137	45	119	41	6
ZSM-5 [27]		*484*	*384*	*264*	*49*	*6*	*3*
Fe-ZSM-5 SSIE		138	124	0	81	32	5

Table 5
Pre-edge peak positions for supported iron samples.

Sample	α-Fe_2O_3	Fe-Beta-75	Fe-ZSM-5	Fe-MCM-41	Fe-SiO_2 (5 wt%)
Pre-edge position (eV)	7113.9	7113.4	7113.6	7113.4	7112.8
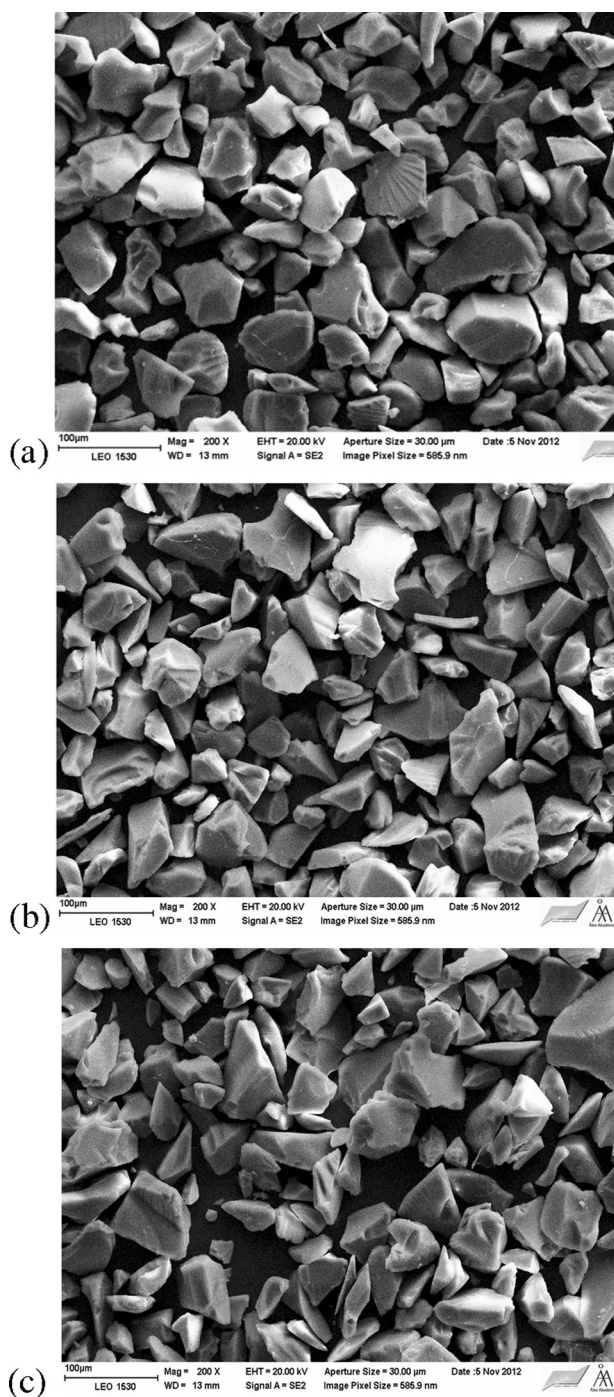
Fig. 4. SEM image of Fe-SiO_2 with loading amount of iron (a) 3 wt.%, (b) 5 wt.% and (c) 10 wt.%.

Fig. 5. SEM image of Fe-Al_2O_3 with loading amount of iron (a) 3 wt.%, (b) 5 wt.% and (c) 10 wt.%.

reported by XPS, but it should be noted that EXAFS gives more in depth results compared to XPS.

The absolute part of the Fourier-transformed k^2-weighted spectra for the samples under study and α-Fe_2O_3 for comparison are presented in Fig. 9. All spectra, including that for the reference oxide, show a signal at distances smaller than 2 Å (uncorrected),

which are attributed to O scatterers. The intensities of this scattering feature are quite similar in most of the samples. The scattering events between 2 and 3.8 Å, which are very intense in α-Fe_2O_3 and arise mostly from Fe neighbors there, are also of low intensity in the silica supported samples. Using those as a particle size indicator, one can conclude that particle size is decreasing in the following sequence: ZSM-5 > MCM-41 > Beta-75 > silica. Fitting results for the
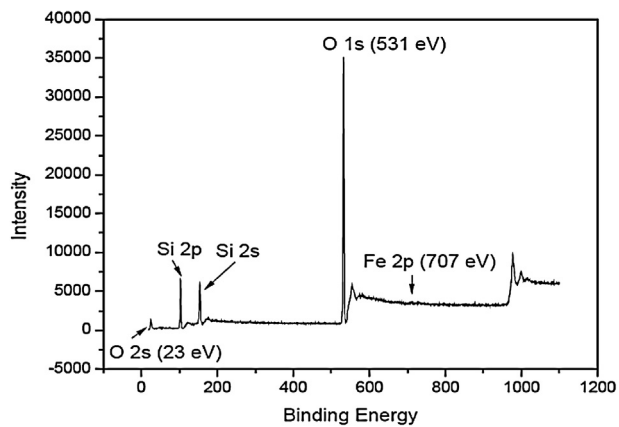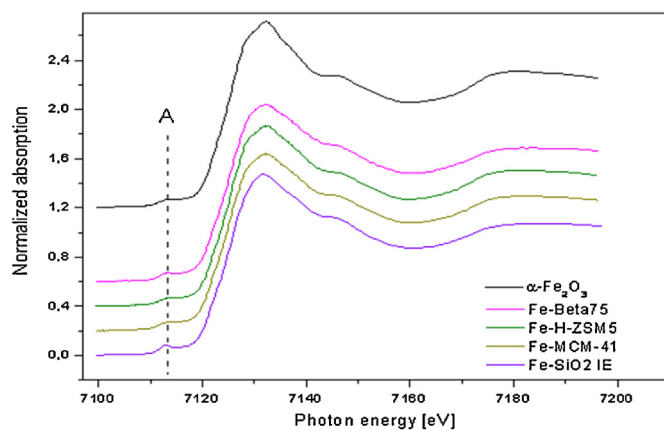
Fig. 6. XPS spectrum of Fe-ZSM-5-SSIE.

Fig. 8. Fe K XANES of Fe-MCM-41-SSIE, Fe-ZSM-5, Fe-Beta-75 and Fe-SiO$_2$ (5 wt.%) compared to α-Fe$_2$O$_3$ reference.
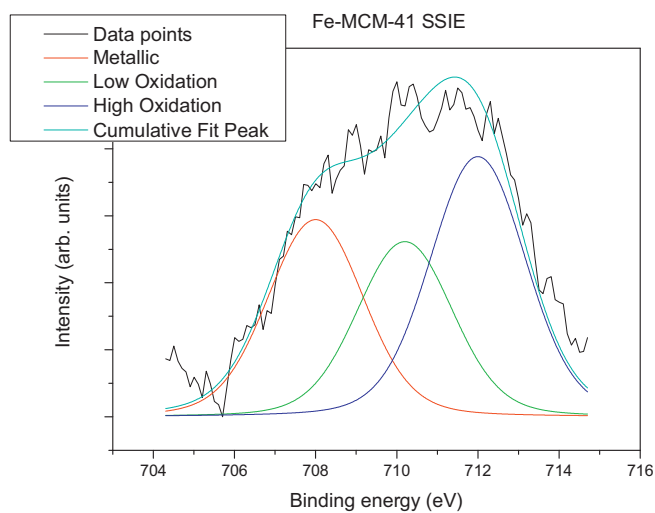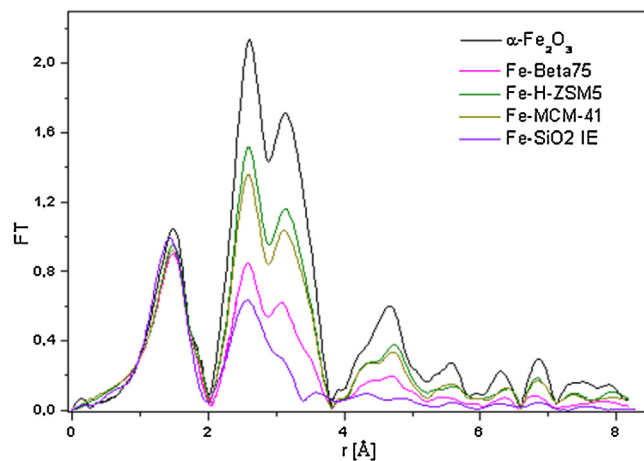

Fig. 7. XPS spectrum with fitted peaks Fe-MCM-41-SSIE.

Fig. 9. EXAFS spectra (modulus of the Fourier-transformed, k^2-weighted spectra) of samples under study compared with reference α-Fe$_2$O$_3$ spectrum.
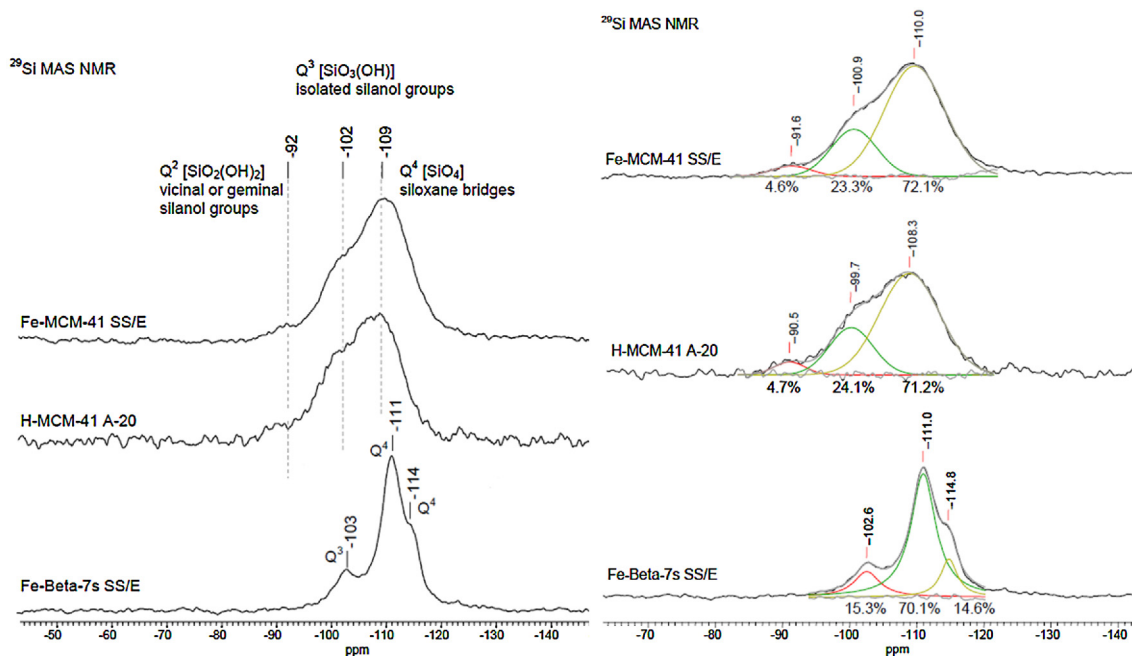

Fig. 10. (a) ^{29}Si MAS NMR spectra of Fe-H-MCM-41 SSIE, proton form of support H-MCM-41 and Fe-Beta-75 SSIE (10 kHz) and (b) its integrated form.

Table 6
Fitting results within 2-shell model.

Catalyst	Shell	CN	r (Å)	σ (10^{-3}Å^{-2})
Fe-Beta-75-SSIE	Fe-O1	3.55 ± 0.72	1.93 ± 0.09	3.82 ± 0.14
	Fe-O2	2.67 ± 0.37	2.07 ± 0.05	3.63 ± 0.88
Fe-ZSM-5-SSIE	Fe-O1	3.82 ± 0.76	1.95 ± 0.09	3.64 ± 0.15
	Fe-O2	2.42 ± 0.82	2.09 ± 0.05	3.66 ± 0.95
Fe-H-MCM-41-SSIE	Fe-O1	3.95 ± 0.77	1.94 ± 0.09	3.50 ± 0.14
	Fe-O2	2.23 ± 0.52	2.08 ± 0.05	3.56 ± 0.88
Fe-SiO$_2$	Fe-O1	3.97 ± 0.11	1.95 ± 0.05	12.70 ± 1.16
	Fe-O2	2.38 ± 0.52	2.02 ± 0.43	18.80 ± 1.17

CN = coordination number.

samples are listed in Table 6. In all cases the sum of the coordination numbers of the first two O shells is close to 6, which confirms the initial conclusion on octahedral iron coordination from XANES analysis.

3.1.6. ^{29}Si MAS NMR and ^{27}Al MAS NMR

Solid state ^{29}Si MAS NMR spectra and ^{27}Al MAS NMR spectra were measured for Fe-H-MCM-41 SSIE, proton form of support H-MCM-41 and Fe-Beta-75 SSIE.

Four different components centered at ∼ −92, ∼ −102, ∼ −110 and ∼ −114 ppm can be distinguished in ^{29}Si MAS NMR spectra of the samples (Fig. 10a).

The spectra of Fe-MCM-41-SSIE and H-MCM-41 exhibited three resonance peaks at −92 ppm, −102 ppm and −109 ppm. The peak signals at −102 ppm and −109 ppm are attributed to the silicon atoms in Q3 [SiO$_3$(OH)] of isolated silanols and Q4 [SiO$_4$] environments of siloxane bridges, respectively. In addition, a small signal attributable to the silicon atoms in Q2 [SiO$_2$(OH)$_2$] environment of vicinal and geminal silanols was also observed at −92 ppm [29].

Fe-Beta-75-SSIE spectrum contains silanol groups which originate resonance peaks at −103 ppm, −111 ppm and −114 ppm. These shifts have been attributed to the Q3 [SiO$_3$(OH)] of isolated silanols and Q4 [SiO$_4$] groups [30].

The ^{27}Al MAS NMR spectra of the samples (Fig. 11) exhibit a resonance peak close to 53 ppm which is attributed to structural tetrahedral coordinated aluminum [29]. The peak around 0 ppm is representative of hexacoordinated aluminum (octahedral coordination) belonging to extra-structural species [29]. Choudhary and Mantri [31] reported that Al present in the framework and extra framework exhibits four and six coordinated states, respectively. In the present study, as the peak intensity for Fe-MCM-41 is more at the octahedral position, most of the Al atoms are present in the extra framework network. In case of Fe-Beta-75, the Al atoms are more present in the tetrahedral forms.

3.1.7. Structural analysis of the catalysts by X-ray powder diffractometer

The structures of Fe-ZSM-5-SSIE, Fe-Beta-75-SSIE, Fe-MCM-41-SSIE, Fe-Al$_2$O$_3$ (3 wt.%) and Fe-SiO$_2$ (3, 5 and 10 wt.%) catalysts have been verified by means of X-ray powder diffraction. The iron oxide peak (Fe$_2$O$_3$) designated at 2θ value of 33° was not observed in the Fe-modified catalysts indicating that either iron was not in crystalline form or Fe particles were small, since they could not be detected by XRD.

As conclusion, iron was in both Fe^{2+} and Fe^{3+} forms in Fe-Beta-75 and Fe-ZSM-5, whereas in addition metallic Fe^0 was present in Fe-MCM-41 according to XPS. Furthermore, iron was in the form of hematite according to EXAFS analysis. The peak signals at −102 ppm and −109 ppm are attributed to the silicon atoms in Q3 [SiO3(OH)] of isolated silanols and Q4 [SiO$_4$] environments of siloxane bridges, respectively. In addition, a small signal attributable to the silicon atoms in Q2 [SiO$_2$(OH)$_2$] environment of vicinal and geminal silanols was also observed at −92 ppm [29].

3.2. Isomerization of α-pinene oxide

3.2.1. Reaction course of α-pinene oxide isomerization

Different iron modified materials with different physico-chemical properties were studied for α-pinene oxide isomerization in this work. The activities and selectivities of all catalysts were mainly correlated with their acid properties and different structures of supports. In addition, the influence of loading amount of iron and the possibility of regeneration of the catalyst were studied.

The results of the catalytic experiments focused on the preparation of campholenic aldehyde by α-pinene oxide isomerization
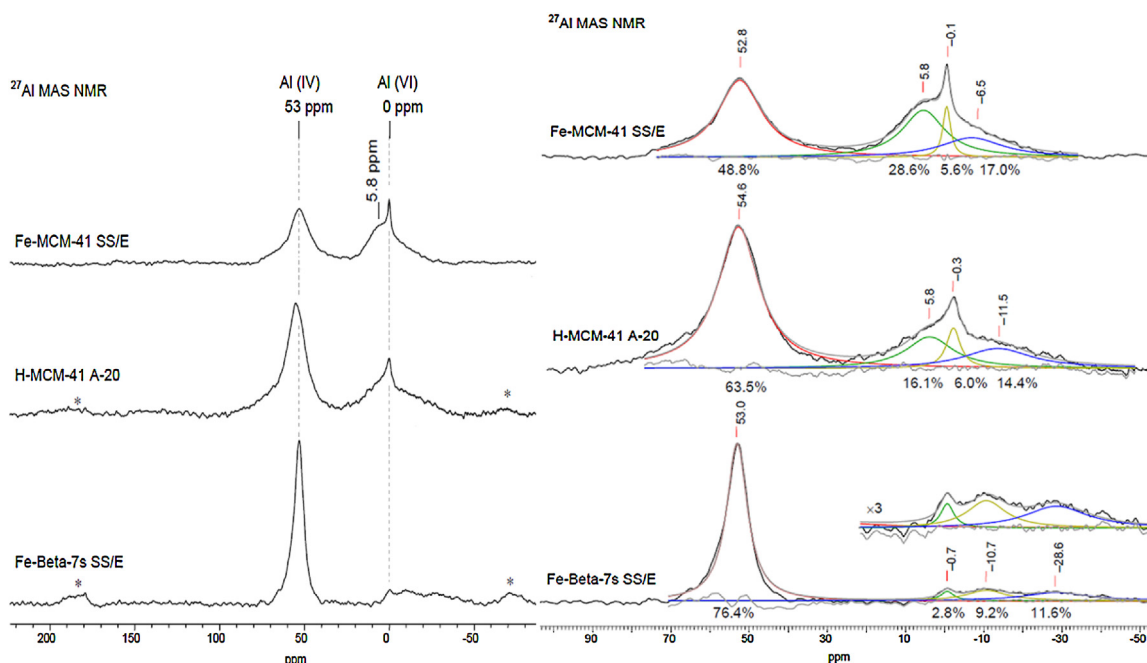
Fig. 11. (a) ^{27}Al MAS NMR spectra of Fe-H-MCM-41 SSIE, proton form of support H-MCM-41 and Fe-Beta-75 SSIE (13 kHz) and (b) its integrated form.

Table 7
Initial reaction rate, conversion of α-pinene oxide and selectivities to the desired campholenic aldehyde at 20% conversion of α-pinene oxide.

Catalyst	Iron content (wt.%)	Initial reaction rate (mmol/L min g_{cat})	Conversion of APO after 3 h (%)	Selectivity to CA at 20% conversion of APO (%) [a] (at 100% conversion)
Fe-SiO$_2$	2.4	3.5	26	71
	4.6	2.6	41	75
	8.3	3.9	55	75
Fe-Al$_2$O$_3$	2.8	2.6	55	56
	4.5	4.1	42	69
	7.1	2.4	43	57
Fe-H-MCM-41-SSIE	2.9	40.0***	100	60* (66) [a]
Fe-Beta-75-SSIE	3.1	46.2***	100	48** (51) [a]
Fe-ZSM-5-SSIE	1.2	4.7	21	52

Reaction conditions: 70 °C, toluene; APO = α-pinene oxide, CA = campholenic alcohol.
*at 60% conversion, ** at 85% conversion, [a] at 100% conversion. ***average rate for the first few minutes.

over iron modified materials are shown in Table 7. The initial reaction rate was calculated according to

$$r_0 = \left(\frac{(c_0 - c_t)}{t} \frac{1}{m_{cat}} \right),$$

where c_0 and c_t are initial and actual concentration of APO (mmol/L), t is reaction time (3 min in this case) and m_{cat} is mass of catalyst (g) (1)

The high initial reaction rates were achieved using Fe-H-MCM-41-SSIE and Fe-Beta-75-SSIE with materials with ordered mesoporous and microporous structure. The highest initial reaction rate, being 46 mmol L^{-1} min^{-1} g$_{cat}$$^{-1}$, was achieved using Fe-Beta-75-SSIE, the catalyst with the highest Lewis and Brønsted acidity. Iron supported on zeolite ZSM-5 exhibited a low initial reaction rate and also a low conversion of α-pinene oxide despite the high amounts of Lewis and Brønsted acid sites. This is because of the structure of this zeolite which is characterized by a very small pore diameter. Iron supported on silica and alumina exhibited low initial reaction rates, which could be explained by a low concentration of Brønsted acid sites and furthermore by low specific surface areas of these catalysts. Among three Fe-Al$_2$O$_3$ catalysts the most active was 5 wt.% Fe-Al$_2$O$_3$ with the highest amount of Lewis and Brønsted acid sites. The lowest initial rate among iron supported on silica catalysts was achieved over 5 wt.% Fe-SiO$_2$.

The total conversion of α-pinene oxide was achieved using Fe-H-MCM-41-SSIE and Fe-Beta-75-SSIE within 20 minutes from the beginning of the reaction.

The highest selectivity to the desired campholenic aldehyde at 20% conversion of α-pinene oxide was obtained using Fe-SiO$_2$ with different loading amounts of iron.

Minor often encountered products are fencholenic aldehyde, *trans*-carveol, isopinocamphone, pinocarveol and *p*-cymene. The product distribution varied over different iron catalysts which will be discussed below.

It can be concluded that the activity of the catalyst increases with the increasing amount of Brønsted acid sites. This corresponds to previously reported results [15] for α-pinene oxide isomerization over iron-modified zeolites under similar reaction conditions. The highest initial rate was achieved using Fe-Y-12 SSIE catalyst, which is characterized by very high concentration of Brønsted acid sites [15]. The complete conversion of α-pinene oxide was achieved using this catalyst with selectivity to campholenic aldehyde 68% at 78% conversion level. On the other hand, it has been earlier reported that the isomerization rates increased with increasing iron loading using Fe on mesoporous silica [14], but in the current study the initial isomerization rate did not depend on the iron loading. It should, however, be pointed out here and the final conversion increased with increasing iron loading showing that the final activity of the catalysts was in line with iron loading. In the case of alumina with different metal loadings, it was shown that with 5 and 10 wt.% Fe the catalyst became magnetic and thus no conclusions can be drawn
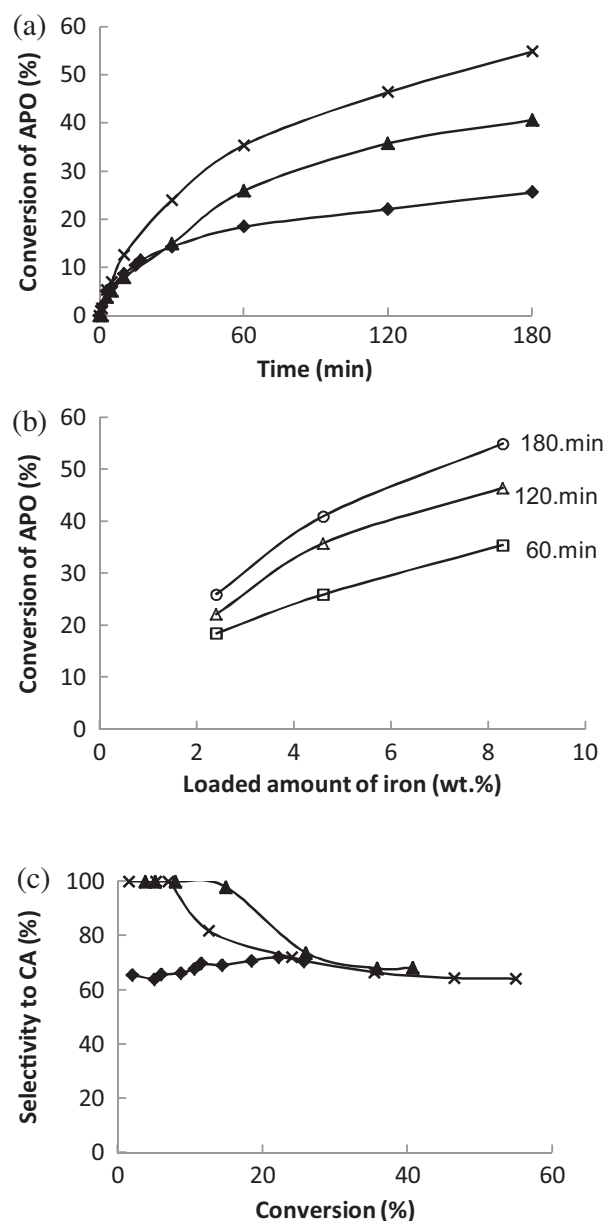
Fig. 12. The conversion of α-pinene oxide at 70 °C in toluene as (a) a function of reaction time and as (b) a function of loaded amount of iron and (c) the selectivity to campholenic aldehyde as a function of the conversion of α-pinene oxide over Fe-SiO$_2$ (3 wt.%) (♦), Fe-SiO$_2$ (5 wt.%) (▲) and Fe-SiO$_2$ (10 wt.%) (X).

Table 8
The selectivities to campholenic aldehyde, fencholenic aldehyde, *trans*-carveol and isopinocamphone over Fe-SiO$_2$ (3, 5 and 10 wt.%) at 25% and 40% conversion of α-pinene oxide.

Catalyst	Iron content (wt.%)	Selectivities (%) at 25% conversion of APO[a] (at 40% conversion)			
		CA	FA	TCV	Isopinocamphone
	3	71	0	15	12
Fe-SiO$_2$	5	75 [a](68)	0 [a](7)	13 [a](13)	12 [a](12)
	10	72 [a](65)	0 [a](8)	16 [a](15)	12 [a](10)

Reaction conditions: 70 °C, toluene; APO = α-pinene oxide, CA = campholenic alcohol, FA = fencholenic aldehyde, TCV = *trans*-carveol; [a]at 40% conversion.

from the iron loading and initial rate dependence using alumina as a support (see below).

3.2.2. Effect of loaded amount of iron on silica

The conversion of α-pinene oxide as a function of the reaction time over Fe supported on silica on the loaded amount of iron is depicted in Fig. 12a. Fig. 12b shows that the conversion of α-pinene oxide increases proportionally with the amount of iron loaded on silica at different reaction time (60, 120 and 180 min).

The selectivity to the desired campholenic aldehyde as a function of conversion of α-pinene oxide is depicted in Fig. 12c. The highest selectivity to the desired aldehyde at 20 % conversion of α-pinene oxide was achieved using Fe-SiO$_2$ (5 wt.%) being 75%. The selectivity to campholenic aldehyde for this catalyst decreased during the reaction and it was 68% at 41% conversion after 180 min from the beginning of the reaction. The selectivity to campholenic aldehyde also decreased during the reaction using Fe-SiO$_2$ (10 wt.%). Only in the case of Fe-SiO$_2$ (3 wt.%) the selectivity slightly increased with increasing conversion of α-pinene oxide. The selectivities to campholenic aldehyde reached the same level at 26% conversion using all three catalyst being 73%.

Trans-carveol and isopinocamphone were the main by-products using Fe-SiO$_2$ catalysts which contain very low amount of Brønsted acidity. According to literature formation of campholenic aldehyde, pinocarveol and isopinocamphone are catalyzed by Lewis acidity [7]. These products were formed from the beginning of the reaction over Fe-SiO$_2$ (3 wt.%). With higher amounts of Fe (5 and 10 wt.%) the formation of by-products started to be observed at conversion of α-pinene oxide 20% and 10%, respectively.

The selectivities to products of α-pinene oxide isomerization over iron modified silica catalysts are shown in Table 8. The highest selectivity to campholenic aldehyde at 25% conversion of α-pinene oxide was obtained with Fe-SiO$_2$ (5 wt.%), being 75%. It decreased, however, with increasing conversion of α-pinene oxide to 68% at 40% conversion of α-pinene oxide, which can be a sign that the amount of different types of active sites changes with time and

iron is not probable very equally distributed as reported in ref. [14]. Fencholenic aldehyde is formed at higher conversions of α-pinene oxide. Formation of *trans*-carveol and isopinocamphone is similar using all three Fe-SiO$_2$ catalysts. Fe-SiO$_2$ with 5 wt.% Fe contained the main part of iron in the state 2+, showing that Fe^{2+} is quite selective for production of campholenic aldehyde analogously to Fe in Fe-Beta-300-IE [15].

The sum of concentrations of C5 aldehydes (campholenic and fencholenic aldehyde), as a function of concentration of uncleaved products (isopinocamphone and pinocarveol) and of concentrations of C6 products (*trans*-carveol) over silica modified catalyst is depicted in Fig. 13. No *p*-cymene was formed with Fe-silica supported catalysts, which exhibited nearly no Brønsted acid sites. The formation of side products is delayed after formation of campholenic aldehyde over catalyst with higher iron contents (5 and 10 wt.%). Otherwise the formation of isopinocamphone and pinocarveol and the formation of *trans*-carveol seem to be almost linear with formation of campholenic and fencholenic aldehyde.

3.2.3. Effect of loaded amount of iron on alumina

The conversion of α-pinene oxide as a function of the reaction time over Fe supported on alumina with loaded amount of iron is depicted in Fig. 14 a. The highest conversion of α-pinene oxide was achieved using Fe-Al$_2$O$_3$ (3 wt.%) being 55% within 180 minutes from the beginning of the reaction. Alumina with higher content of iron (5 and 10 wt.%) showed high magnetism and because of that fact the catalyst remained on the thermocouple and was not well stirred in the reaction mixture. This fact caused that the conversions obtained using these catalyst were lower, 42% and 43%, respectively.

The selectivities to the desired campholenic aldehyde as a function of conversion of α-pinene oxide are shown in Fig. 14b. The selectivity to campholenic aldehyde decreased with increasing conversion of α-pinene oxide using all Fe-Al$_2$O$_3$ catalysts because of by-products formation.
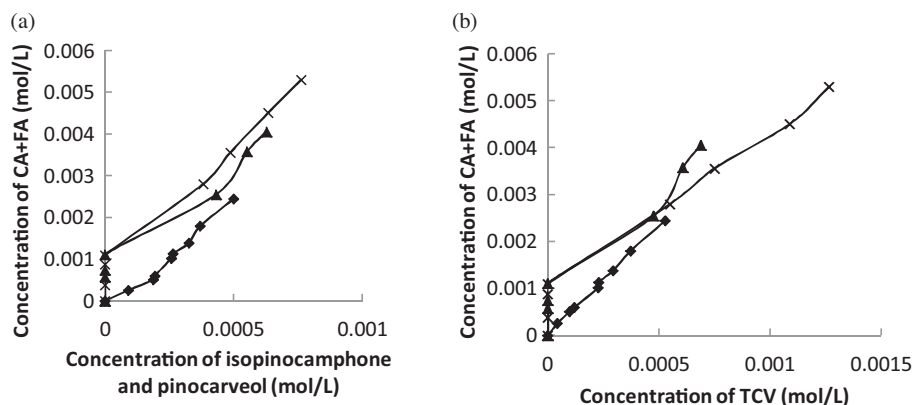
Fig. 13. The concentration of campholenic and fencholenic aldehyde as a function of (a) concentration of isopinocamphone and pinocarveol and as a function of (b) concentration of *trans*-carveol over Fe-SiO$_2$ (3 wt.%) (♦), Fe-SiO$_2$ (5 wt.%) (▲) and Fe-SiO$_2$ (10 wt.%) (X).
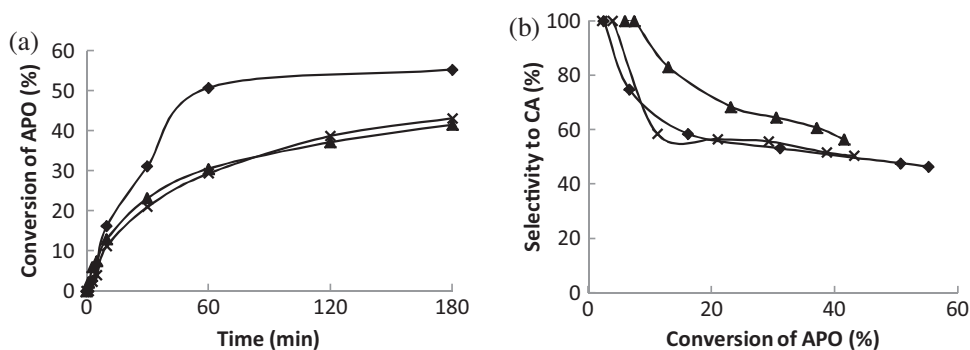
Fig. 14. (a) The conversion of α-pinene oxide as a function of reaction time and (b) the selectivity to campholenic aldehyde as a function of the conversion of α-pinene oxide over Fe-Al$_2$O$_3$ (3 wt.%) (♦), Fe-Al$_2$O$_3$ (5 wt.%) (▲) and Fe-Al$_2$O$_3$ (10 wt.%) (X).

Table 9
Selectivities to campholenic aldehyde, fencholenic aldehyde, isopinocamphone and pinocarveol over Fe-Al$_2$O$_3$ (3, 5 and 10 wt.%) at 40% conversion of α-pinene oxide.

Catalyst	Iron content (wt.%)	Selectivities at 40% conversion of APO (%)			
		CA	FA	Isopinocamphone	Pinocarveol
	3	51	5	19	26
Fe-Al$_2$O$_3$	5	58	2	17	23
	10	51	4	17	28

Reaction conditions: 70 °C, toluene; APO = α-pinene oxide, CA = campholenic alcohol, FA = fencholenic aldehyde, TCV = *trans*-carveol.

Isopinocamphone and pinocarveol were the main by-products using Fe-Al$_2$O$_3$ catalysts. Characteristic for these products is that they are formed by opening only epoxide ring of α-pinene oxide (Fig. 1). The selectivity to campholenic aldehyde was thus lower because of their formation than with other types of catalysts being below 60% for all Fe-Al$_2$O$_3$ catalysts. The selectivities towards α-pinene oxide isomerization products over iron modified alumina catalysts are compared in Table 9.

3.2.4. Effect of various structures of micro- and mesoporous supports

The conversion of α-pinene oxide as a function of reaction time over Fe supported on MCM-41 mesoporous material and Beta-75 and ZSM-5 zeolites is illustrated in Fig. 15a. The complete conversion of α-pinene oxide was achieved using Fe-Beta-75-SSIE and Fe-MCM-41-SSIE within 20 min from the beginning of the reaction. The conversion for Fe-ZSM-5-SSIE was the lowest from all iron supported catalysts being only 21% after 180 min of time. All these support as well as iron modified supports exhibited high surface areas. Since ZSM-5 is characterized by small pore diameter (0.5 nm), it is usually not suitable for preparation of specialty chemicals with larger kinetic diameter. α-Pinene oxide is a relatively large molecule not fitting to the pores of zeolite ZSM-5 therefore

its isomerization proceeds only on the external catalysts surface and not in its pores.

The selectivity to the desired campholenic aldehyde as a function of conversion of α-pinene oxide is demonstrated in Fig. 15b. This figure shows that the selectivity to campholenic aldehyde slightly increases with increasing conversion of α-pinene oxide for all three iron containing catalysts.

The other by-products formed using iron supported on ordered materials were fencholenic aldehyde, *trans*-carveol, *p*-cymene, isopinocamphone and pinocarveol. The selectivities to campholenic aldehyde and to the by-products of α-pinene oxide isomerization over iron modified ordered supports are shown in Table 10. The highest selectivity to the desired campholenic aldehyde was obtained over Fe-MCM-41-SSIE being 66% at total conversion of α-pinene oxide. It should also be pointed out that with Fe-MCM-41-SSIE a relatively constant selectivity with conversion was obtained opposite to the results with Fe-silica or alumina. The lowest selectivity to campholenic aldehyde was exhibited by Fe-Beta-75-SSIE at total conversion of α-pinene oxide at the expense of the isomer, fencholenic aldehyde, formed with the higher selectivity using this catalyst. It should be pointed out here, that this catalyst exhibited the highest Brønsted acidity (Table 2) and thus lower selectivity was achieved with this catalyst compared
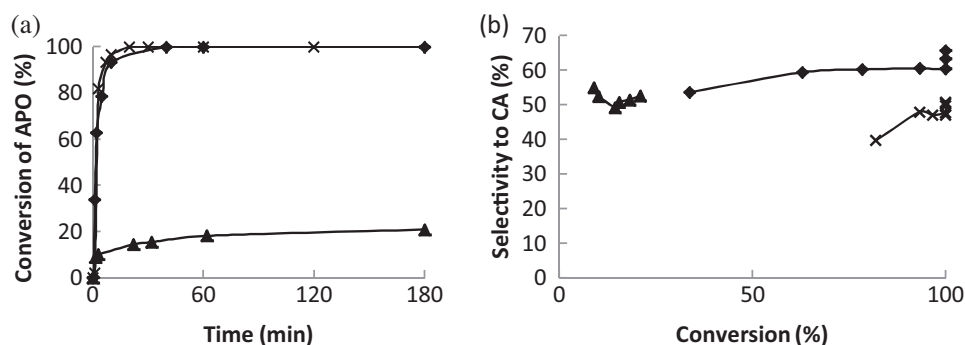
Fig. 15. (a) The conversion of α-pinene oxide at 70 °C in toluene as a function of reaction time and (b) the selectivity to campholenic aldehyde as a function of the conversion of α-pinene oxide over Fe-MCM-41-SSIE (♦), Fe-ZSM-5 (▲) and Fe-Beta-75 (X).

Table 10
The selectivities to campholenic aldehyde, fencholenic aldehyde, *trans*-carveol, *p*-cymene, isopinocamphone and pinocarveol over Fe-ZSM-5, Fe-Beta-75 and Fe-MCM-41 at 20% (Fe-ZSM-5), 90% and 100% (Fe-Beta-75, Fe-MCM-41) conversion of α-pinene oxide.

Catalyst	Selectivities at 20*/90** % conversion of APO [a] (at 100% conversion)					
	CA	FA	TCV	*p*-cymene	Isopinocamphone	Pinocarveol
Fe-ZSM-5-SSIE *	52	9	13	3	8	4
Fe-Beta-75-SSIE **	45 [a](51)	21 [a](23)	12 [a](2)	4 [a](10)	3 [a](4)	1 [a](0)
Fe-MCM-41-SSIE **	60 [a](66)	8 [a](9)	16 [a](0)	4 [a](8)	4 [a](6)	1 [a](0)

Reaction conditions: 70 °C, toluene; APO = α-pinene oxide, CA = campholenic alcohol, FA = fencholenic aldehyde, TCV = *trans*-carveol; * 20% conversion of APO, ** 90% conversion of APO.

to Fe-MCM-41-SSIE and Fe-ZSM-5-SSIE catalysts with lower amounts of Brønsted acid sites. Iron was mainly in the oxidation state of 3+ in Fe-MCM-41-SSIE, although also Fe^0 and 2+ Fe were present (Table 3).

When comparing these selectivities with the ones achieved with Fe-SiO₂ and comparing the state of iron in Table 3, it is not easy to make definite conclusions of the state of iron needed for selective isomerization of α-pinene oxide to campholenic aldehyde. Selectivities to campholenic acid reported with iron supported on mesoporous silica were about 53% in toluene at 25 °C [14] and in their work iron was present in Fe₂O₃ and as FeOx as well as in a metallic form. On the other hand, the presence of an adequate amount of Lewis acid and a relatively low concentration of Brønsted acid sites are beneficial. One exception has been, however, observed in the catalyst screening for isomerization of α-pinene oxide to campholenic aldehyde, namely Fe-Y-12-SSIE, which exhibited also high Brønsted acidity and relatively high selectivity to campholenic aldehyde, 68% at 78% conversion [15] under similar conditions as used here thus showing that the zeolite structure can also affect selectivity. It should be noted that the presence of iron is essential for obtaining high selectivity to campholenic aldehyde. For example in case of parent H-Y-12 the maximum selectivity to campholenic aldehyde is only 42%, while selectivity to *p*-cymene reaches 19%. Moreover, large amounts of isopinocamphone (selectivity 27%) were observed for this catalyst.

Trans-carveol was formed during the isomerization reactions using all three catalysts. It was further transformed via dehydration and dehydrogenation mainly to *p*-cymene for catalysts with higher activity (Fe-Beta-75-SSIE, Fe-MCM-41-SSIE). The formation of *p*-cymene increased with increasing conversion being 10% and 8% at the total conversion of α-pinene oxide over

Fe-Beta-75-SSIE and Fe-MCM-41-SSIE, respectively. This result shows that higher Brønsted acidity leads to higher *p*-cymene formation with Fe-Beta-75-SSIE compared to Fe-MCM-41-SSIE, although the difference is not very high. Furthermore, *p*-cymene formation is easier using a mesoporous Fe-MCM-41-SSIE catalyst showing that the Brønsted acidity of Fe-MCM-41-SSIE is high enough to catalyze dehydration. Analogously to these results also quite large amounts of *p*-cymene were formed with mildly Fe-Beta-300-IE catalyst in [15] showing that an adequate amount of Brønsted acidity is required.

Fig. 16 displays concentration of all products over the most active catalysts Fe-MCM-41-SSIE (Fig. 16a) and Fe-Beta-75-SSIE (Fig. 16b) using toluene as a solvent. The initial concentration of substrate was 0.013 mol/l. The mass balance closure of compounds in 180 min is 92% using Fe-Beta-75 and 85% using Fe-MCM-41.

The ratio between campholenic and fencholenic aldehydes remained at the same level during the reaction over Fe-MCM-41-SSIE, Fe-Beta-75-SSIE and Fe-ZSM-5-SSIE (Fig. 17a). Nearly linear parallel formation of these products can be observed using all catalysts independent on the support structure. The formation of *trans*-carveol and its further transformation via dehydration and dehydrogenation to *p*-cymene are shown in Fig. 17b. *Trans*-carveol is totally transformed to *p*-cymene over Fe-MCM-41-SSIE and Fe-Beta-75-SSIE.
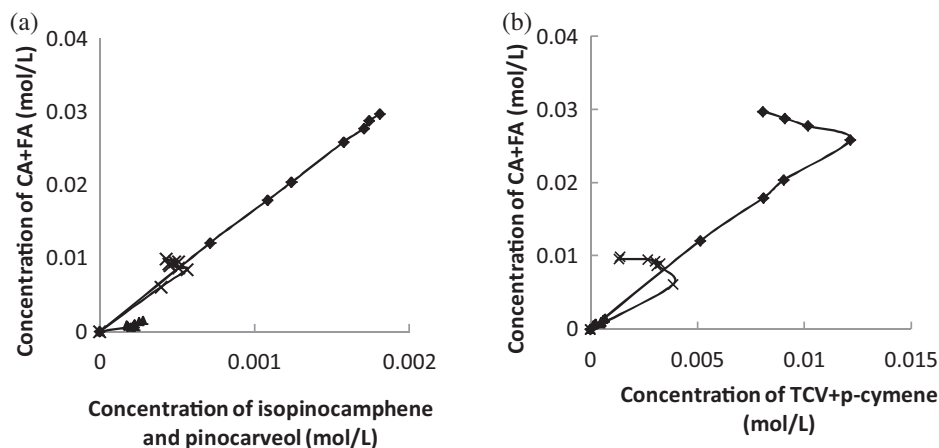
The sum of concentrations of campholenic and fencholenic aldehyde (C5 aldehydes) as a function of concentration of isopinocamphone and pinocarveol (uncleaved products) and of concentrations of *trans*-carveol and *p*-cymene (C6 products) over iron modified ordered materials is depicted in Fig. 18. The formation of side uncleaved products isopinocamphone and pinocarveol is linear with formation of campholenic and fencholenic aldehyde
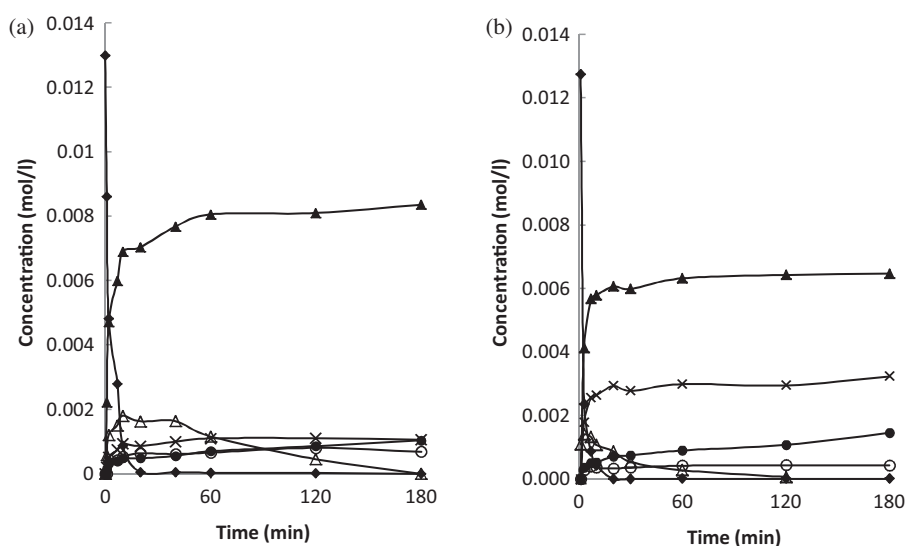
Fig. 16. Kinetics in the α-pinene oxide isomerization over **(a)** Fe-MCM-41-SSIE and **(b)** Fe-Beta-75-SSIE at 70 °C, using toluene as a solvent. Symbols: α-pinene oxide (♦), campholenic aldehyde (▲), fencholenic aldehyde (X), *p*-cymene (●), *trans*-carveol (△) and isopinocamphone (o).
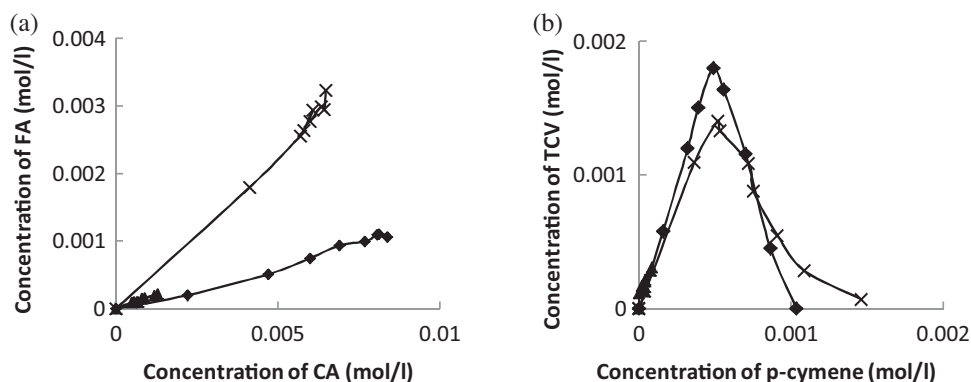
Fig. 17. (a) Concentration of fencholenic aldehyde versus concentration of campholenic aldehyde and (b) concentration of *trans*-carveol versus concentration of *p*-cymene over Fe–MCM-41-SSIE (♦), Fe–ZSM-5-SSIE (▲) and Fe–Beta-75-SSIE (X).

Fig. 18. The concentration of campholenic and fencholenic aldehyde as a function of (a) concentration of isopinocamphone and pinocarveol and as a function of (b) concentration of *trans*-carveol and *p*-cymene over Fe–MCM-41-SSIE (♦), Fe–ZSM-5-SSIE (▲) and Fe–Beta-75-SSIE (X).

during the reaction over Fe-MCM-41-SSIE and Fe-ZSM-5-SSIE (Fig. 18a) pointing out on the parallel reaction network. Interestingly the ratio is not influenced by the structure of support. In the case of Fe-Beta-75-SSIE, the concentration of isopinocamphone and pinocarveol does not increase after 10 min from the beginning of the reaction. These products are probably transformed further (Fig. 18a).

Fig. 18b shows parallel formation of *trans*-carveol and *p*-cymene with formation of campholenic and fencholenic aldehyde at the beginning of the reaction over all three catalysts. *Trans*-carveol reacts further to *p*-cymene as was shown above (Fig. 17b). Despite the fact that *p*-cymene is a very stable product, its concentration decreases at higher conversions of α-pinene oxide over Fe-Beta-75-SSIE and Fe-MCM-41-SSIE most probably due to its further transformations to coke.

3.2.5. Influence of Lewis and Brønsted acid sites of the catalysts on the product formation

As discussed above, the acidity of catalysts influenced the activity and mainly the selectivity of them. It was concluded, that the presence of an adequate amount of Lewis acid and a relatively low concentration of Brønsted acid sites are beneficial. The influence of the Lewis acid sites on the formation of campholenic aldehyde is depicted in Fig. 19 (a). Lewis acid sites can react with the oxygen atom of epoxide ring causing than splitting of adjacent C–C bond in 6-member carbon-ring forming thereby desired campholenic aldehyde. On the other hand, Fig. 19b shows a possible interaction of

Brønsted acid sites represented by H⁺ atom with α-pinene oxide and a mechanism of *trans*-carveol formationf.

3.2.6. Possibilities of the catalyst Fe-MCM-41-SSIE reuse and regeneration

The most active and the most selective catalyst, Fe-MCM-41-SSIE, was further tested to determine its possible regeneration and reuse. The results of the catalytic experiments focused on the preparation of campholenic aldehyde by α-pinene oxide isomerization over fresh, spent and regenerated Fe-MCM-41-SSIE materials are shown in Table 11.

The total conversion of α-pinene oxide was achieved using all three catalysts despite the fact that reused and regenerated catalysts exhibited lower surface areas (Table 2). The highest initial reaction rate was achieved using fresh Fe-MCM-41 although it is comparable to the initial reaction rate obtained using regenerated catalyst. The activity in the case of the reused catalyst was lower because some pore blocking occurred.

The selectivities to the desired campholenic aldehyde at 100% conversion of α-pinene oxide decreased slightly from 66% with the fresh catalyst to 64% for the regenerated one and to 59% for the reused one.

The conversion of α-pinene oxide as a function of reaction time over Fe-MCM-41-SSIE catalysts is demonstrated in Fig. 20a. The total conversion of α-pinene oxide was achieved using the fresh and regenerated Fe-MCM-41-SSIE catalysts in 30 min. Reused catalyst exhibited decrease of its activity by about 30%. The total conversion
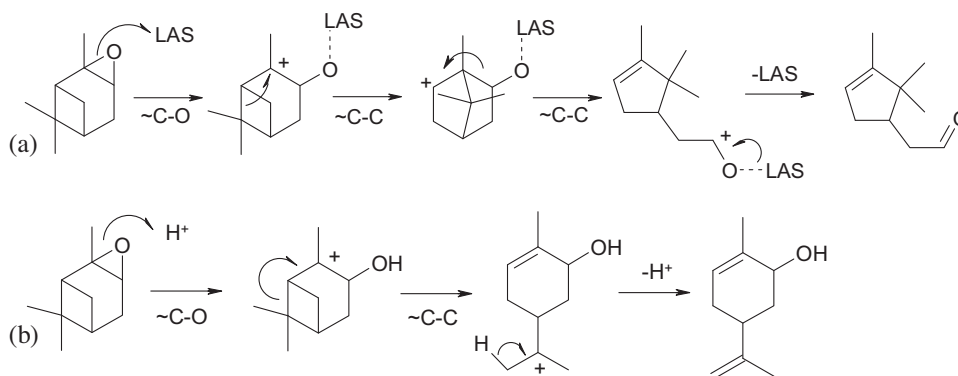
Fig. 19. Formation of (a) campholenic aldehyde over Lewis acids sites and (b) *trans*-carveol over Brønsted acid sites.

Table 11
Initial reaction rate, conversion of α-pinene oxide and selectivities to campholenic aldehyde at 60% and 100% conversion of α-pinene oxide over fresh, regenerated and spent Fe-MCM-41-SSIE catalysts.

Catalyst	Initial reaction rate (mmol/min g_{cat})	Conversion of APO after 3 h (%)	Selectivity to CA	
			at 60% conversion of APO (%)	at 100% conversion of APO (%)
Fe-H-MCM-41-SSIE fresh	45.2	100	60	66
Fe-H-MCM-41-SSIE regenerated	42.7	100	63	64
Fe-H-MCM-41-SSIE spent	15.9	100	59	59

Reaction conditions: 70 °C, toluene; APO = α-pinene oxide, CA = campholenic alcohol.

over the reused Fe-MCM-41-SSIE was obtained after 180 minutes. The activity decrease of the reused catalyst can be caused by the deactivation of the Brønsted acidic centers responsible for α-pinene oxide transformation which can be than reactivated by the regeneration.

The selectivity to campholenic aldehyde as a function of α-pinene oxide conversion over fresh Fe-MCM-41-SSIE is compared with the regenerated and with the reused catalysts in Fig. 20b. It can be seen that the selectivity to campholenic aldehyde does not change with the deactivation of the catalysts.

Results in the current work correspond well with the in-depth study of Gervasini et al. [14] on the influence of iron content on α-pinene oxide isomerization using oxide catalysts with highly dispersed Fe phases supported on a mesoporous, high surface silica (Fe/SIM). The iron was in a wide range of concentration (4 < Fe2O3 mass% < 17) [14]. It was reported that reaction rates increased with the increase of Fe loading [14]. In the current study the initial reaction rates did not depend on the iron loading. But the isomerization rates during the reaction increased with increasing iron loading for Fe-SiO2 (Fig. 12) and also final activity of the catalysts was in line with iron loading.

Conclusions of the present study, that the presence of an adequate amount of Lewis acid and a relatively low concentration of Brønsted acid sites is beneficial for campholenic aldehyde formation, are in accordance with conclusions of reported results of Ravasio et al. [16]. In the latter work, iron were supported onto pure silica and a series of modified silicas with variable amounts of zirconia (5–45 mass% of ZrO2) and tested in α-pinene oxide isomerization [16]. The best selectivity to campholenic aldehyde was observed over Fe supported on pure silica, i.e. the least active catalysts. Introduction of zirconia into the support led to an increase in activity together with a decrease in selectivity, showing the contribution of Brønsted acidity from the support. Fe/SZ5 represented the best compromise between activity and selectivity and using this catalysts total conversion of α-pinene oxide with 65% selectivity to campholenic aldehyde was obtained in toluene at room temperature [16]. The main disadvantage of this catalyst is again the necessary amount of catalysts added to the reaction in ratio 1:1 to substrate. Furthermore, analysis data (EDXA) confirmed iron leaching from the solid supports under experimental conditions. Because of this fact, recycling of the catalysts is not possible. Conclusion that the activity of the catalyst increases with the increasing
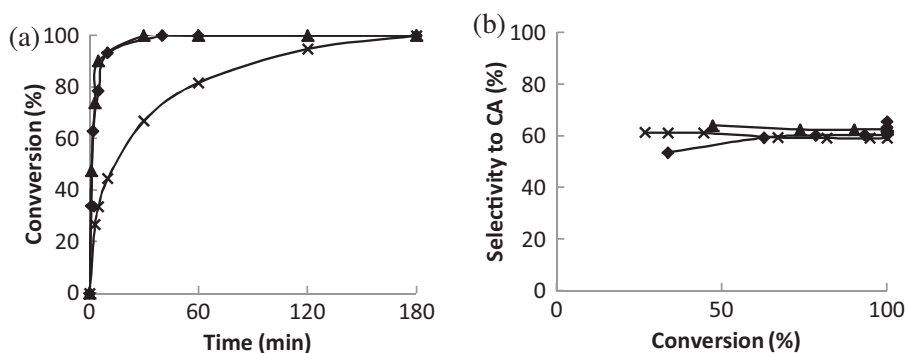

Fig. 20. (a) The conversion of α-pinene oxide at 70 °C in toluene as a function of reaction time and (b) the selectivity to campholenic aldehyde as a function of the conversion of α-pinene oxide over Fe-MCM-41-SSIE fresh (♦), Fe-MCM-41-SSIE regenerated (▲) and Fe-MCM-41-SSIE spent (X).

amount of Brønsted acid sites was also previously reported [15] for α-pinene oxide isomerisation over iron-modified zeolites under similar reaction conditions. The highest initial rate was achieved using Fe-Y-12 SSIE, the catalyst characterized by very high concentration of Brønsted acid sites [15].

The state of iron has been reported to affect the isomerization rate [17]. Slightly higher activities of iron modified MCM-41 were achieved when the catalyst contained iron in Fe^{3+} state compared to Fe^{2+} state [17]. Conversion level of 94% of α-pinene oxide was obtained using Fe^{3+}-MCM-41 in acetone as a solvent at 40 °C within 3 hours from the beginning of the reaction. Analogously to the results of Coelho et al. [17] in the current work the high isomerization rates were observed with Fe-Beta-75-SSIE and Fe-MCM-41-SSIE, in which 50% and 41% of iron was in the state 3^+ (Table 3).

The high selectivity up to 89% to campholenic aldehdyde was reported over Lewis acid catalysts Ti-Beta with Si/Ti ratio of 59 (aluminum-free catalysts) using solvents with various polarity [8]. This high selectivity was achieved using acetonitrile but the catalysts deactivated rapidly, resulting in a conversion of only 7% after 24 h [8]. Toluene, solvent tested in the present study, can be compared with benzene from the viewpoint of these solvents similar polarity. Dielectric constants of benzene and toluene are 2.28 and 2.38, respectively. Conversion of α-pinene oxide over Ti-Beta using benzene was only 35% after 24 hours with selectivity 55% to campholenic aldehyde [8]. Better results were shown in the present study, because conversion of α-pinene oxide over Fe-Beta-75 using toluene was 100% after 20 minutes with selectivity 51% to campholenic aldehyde.

4. Conclusions

Bifunctional catalysts exhibiting both Lewis and Brønsted acidity and different structures Beta-75 and ZSM-5 zeolites, MCM-41 mesoporous material modified with Fe using solid state ion-exchange method were studied in selective isomerization of α-pinene oxide. Comparative experiments with $Fe-SiO_2$ and Fe-Al_2O_3 catalysts were also performed to study the influence of support in the α-pinene oxide isomerization. The aim was to elucidate the nature of active sites, effect of acidity, support and catalyst structure. The possibility of heterogeneous catalyst (Fe-H-MCM-41-SSIE) regeneration without activity loss was demonstrated.

Isomerization of α-pinene oxide at 70 °C using toluene as a solvent shows that the main parameters influencing the activity and selectivity to campholenic aldehyde are the amount and type of Brønsted and Lewis acid sites, content of Fe, method of introduction of Fe, type of support and structural properties of the catalysts. The total conversion of α-pinene oxide was achieved using materials with ordered mesoporous and microporous structure Fe-H-MCM-41 and Fe-Beta-75. The highest activity was exhibited by Fe-Beta-75, the catalyst with the highest concentration of Lewis and Brønsted acid sites. On the other hand, the lowest selectivity to campholenic aldehyde was displayed using this highly acidic catalyst.

During α-pinene oxide isomerization besides campholenic aldehyde also fencholenic aldehyde, *trans*-carveol, isopinocamphone, pinocarveol and *p*-cymene were formed. The highest selectivity to the desired campholenic aldehyde at total conversion of α-pinene oxide was obtained over Fe-MCM-41 being 66%.

The most active and selective catalyst, Fe-MCM-41-SSIE, was tested for its possible regeneration and reuse. The activity obtained for the fresh Fe-MCM-41 is comparable with the regenerated catalyst. The activity decrease of the reused catalyst can be caused by

deactivation of Brønsted acidic centers responsible for α-pinene oxide transformation which can be than be reactivated by regeneration. The selectivity to campholenic aldehyde does not change with catalyst deactivation.

References

[1] P. Mäki-Arvela, I. Simakova, T. Salmi, D.Yu. Murzin, Review in Catalytic Process Development for Renewable materials Chapter 13, Wiley, Imhof (Ed.), 2012.

[2] P. Mäki-Arvela, N. Kumar, S. Faten Diaz, A. Aho, M. Tenho, J. Salonen, A.-R. Leino, K. Kordas, P. Laukkanen, J. Dahl, I. Sinev, T. Salmi, D.Yu. Murzin, J. Mol. Catal. A. Chem. 366 (2013) 228–237.

[3] M. Stekrova, N. Kumar, P. Mäki-Arvela, A. Aho, J. Linden, K. Volcho, N.F. Salakutdinov, D.Yu. Murzin, Opening of monoterpene epoxide to a potent anti-Parkinson compound of paramenthane structure over heterogeneous catalysts, Reac. Kinet. Mech. Cat. (2013), 10.1007, 1114-013-0615-9.

[4] B. Arbusow, Chem. Ber. 68 (1935) 1430–1435.

[5] K. Arata, K. Tanabe, Chem. Lett. (1979) 1017–1018.

[6] J. Kaminska, M.A. Schwegler, A.J. Hoefnagel, H. van Bekkum, Rec. Trav. Chim. Pays Bas 111 (1992) 432–437.

[7] W.F. Hölderich, J. Röseler, G. Heitmann, A.T. Liebens, Catal. Today 37 (1997) 353–366.

[8] P.J. Kunkeler, J.C. Van der Vaal, J. Bremmer, B.J. Zuurdeeg, R.S. Downing, H. van Bekkum, Catal. Lett. 53 (1998) 135–138.

[9] L. Alaerts, E. Seguin, H. Poelman, F. Thibault-Starzyk, P.A. Jacobs, D.E. De Vos, Chem. Eur J. 12 (28) (2006) 7353–7363.

[10] G. Neri, G. Rizzo, C. Crisafulli, L. De Luca, A. Donato, M.G. Musolino, R. Pietropaolo, Appl. Catal., A: Gen. 295 (2) (2005) 116–125.

[11] Y.W. Suh, N. Kim, W.S. Ahn, H.K. Rhee, J. Mol. Catal. A: Chem. 198 (1–2) (2003) 309–316.

[12] K. Wilson, A. Renson, J.H. Clark, Catal. Lett. 61 (1–2) (1999) 51–55.

[13] D.B. Ravindra, Y.T. Nie, S. Jaenicke, G.K. Chuah, Catal. Today 96 (3) (2004) 147–153.

[14] A. Gervasini, C. Messi, P. Carniti, A. Ponti, N. Ravasio, F. Zaccheria, J. Catal. 262 (2009) 224–234.

[15] N. Kumar, P. Mäki-Arvela, S.F. Diáz, A. Aho, Y. Demidova, J. Linden, A. Shepid-chenko, M. Tenhu, J. Salonen, P. Laukkanen, A. Lashkul, J. Dahl, I. Sinev, A.-R. Leino, T. Salmi, D.Yu. Murzin, Top. Catal. 56 (2013) 696–713.

[16] N. Ravasio, F. Zaccheria, A. Gervasini, C. Messi, Catal. Commun. 9 (2008) 1125–1127.

[17] J.V. Coelho, A.L.P. de Meireles, K.A. da Silva Rocha, M.C. Pereira, L.C.A. Oliviera, E.V. Gusevskaya, Appl. Catal., A: Gen. 443–444 (2012) 125–132.

[18] K.M. Reddy, C. Song, Catal. Lett. 36 (1996) 103–109.

[19] N. Kumar, E. Leino, P. Mäki-Arvela, A. Aho, M. Käldström, M. Tuominen, P. Laukkanen, K. Eränen, J.-P. Mikkola, T. Salmi, D.Yu. Murzin, Microp. Mesop. Mater 152 (2012) 71–77.

[20] D. Kubicka, N. Kumar, P. Mäki-Arvela, M. Tiitta, V. Niemi, T. Salmi, D.Yu Murzin, J. Catal. 222 (2004) 65–79.

[21] C.A. Emeis, J. Catal. 141 (1993) 347–354.

[22] K.V. Klementiev, J. Phys. D: Appl. Phys. 34 (2001) 209–217 www.cells.es/Beamlines/CLAESS/software/viper.html

[23] A.L. Ankudinov, B. Ravel, J.J. Rehr, S.D. Conradson, Phys. Rev. B 58 (1998) 7565–7576.

[24] M. Käldström, N. Kumar, T. Heikkilä, M. Tiitta, T. Salmi, D.Yu. Murzin, Chem-CatChem 2 (2011) 539–546.

[25] K. Woo, H.J. Lee, J.P. Ahn, S. Park, Adv. Mater. 15 (20) (2003) 1761–1763.

[26] S.F. Diaz, M.Sc. Thesis, Åbo Akademi, 2012.

[27] N. Kumar, P. Mäki-Arvela, S.F. Diaz, A. Aho, Y. Demidova, J. Linden, A. Shepid-chenko, M. Tenho, J. Salonen, P. Laukkanen, A. Lashkul, J. Dahl, I. Sinev, A.-R. Leino, T. Salmi, D.Yu. Murzin, Top. Catal. 56 (2013) 696–713.

[28] M. Wilke, F. Farges, P.-E. Petit, G.E. Brown Jr., F. Martin, Am. Mineral. 86 (2001) 714–730.

[29] R.A.A. Melo, M.V. Giotto, J. Rocha, E.A. Urquieta-González, Mater. Res. 2 (1999) 173–179.

[30] J. Péraz-Pariente, J. Sanz, V. Fornés, A. Corma, J. Catal. 124 (1990) 217–223.

[31] V.R. Choudhary, K. Mantri, Langmuir 16 (2000) 8024–8030.